Evidence through Mössbauer spectroscopy of two different states for ^{57}Fe probe atoms in $RNiO_3$ perovskites with intermediate-size rare earths, R = Sm,Eu,Gd,Dy

2007 J. Phys.: Condens. Matter 19 036201

(http://iopscience.iop.org/0953-8984/19/3/036201)

INSTITUTE OF PHYSICS PUBLISHING JOURNAL OF PHYSICS: CONDENSED MATTER

J. Phys.: Condens. Matter **19** (2007) 036201 (12pp) doi:10.1088/0953-8984/19/3/036201

Evidence through Mössbauer spectroscopy of two different states for ^{57}Fe probe atoms in $RNiO_3$ perovskites with intermediate-size rare earths, R = Sm, Eu, Gd, Dy

I Presniakov[1], A Baranov[1,2], G Demazeau[2], V Rusakov[1], A Sobolev[1], J A Alonso[3], M J Martínez-Lope[3] and K Pokholok[1]

[1] Department of Chemistry, Lomonosov University, 119992 Moscow, Russia
[2] Institut de Chimie de la Matière Condensée de Bordeaux (ICMCB), UPR-CNRS 9048, 87 Avenue du Dr A Schweitzer, 33608 Pessac Cedex, France
[3] Instituto de Ciencia de Materiales de Madrid, CSIC, Cantoblanco, E-28049 Madrid, Spain

Received 28 September 2006, in final form 13 November 2006
Published 5 January 2007
Online at stacks.iop.org/JPhysCM/19/036201

Abstract

In the present work, ^{57}Fe probe Mössbauer spectroscopy was developed to study the nickelates $RNi_{0.98}Fe_{0.02}O_3$ (R = Sm, Eu, Gd, Dy) with the perovskite-like structure. The restoration method for a distribution function $P(v)$ of the positions (v) involving individual Lorentzian lines has been used for processing and analysing the Mössbauer spectra. The $P(v)$ profile for the nickelates, at $T < T_{IM}$ (T_{IM} corresponding to the transition temperature from insulator to metal), can be described as a superposition of two symmetric peaks with different intensities. The distance between these peaks monotonically increases with the decreasing ionic radius value of the R^{3+} cations (Sm → Gd). The observed asymmetry of the $P(v)$ profile indicates that ^{57}Fe atoms used as a Mössbauer probe are simultaneously stabilized in two non-equivalent crystallographic positions. This result is an indirect evidence for the existence of two types of nickel position in the insulating state of nickelate $RNiO_3$ lattices with intermediate R^{3+} size, which remained questionable from diffraction methods.

1. Introduction

Perovskite-like nickelates $RNiO_3$ (R = rare earth, Y, Tl), with the Ni^{3+} cations being characterized by the low-spin configuration ($t_{2g}^6 e_g^1$), exhibit two reversible phase transitions: an insulator ↔ metal transition at T_{IM} and an antiferromagnetic ↔ paramagnetic transition at T_N [1–3]. The transition temperature (T_{IM}) increases with the decreasing size of the R^{3+} ions, showing a transition from itinerant ($LaNiO_3$) to localized ($LuNiO_3$) e_g^1 electronic behaviour versus the increment of the structural distortion [4]. For nickelates with the largest R^{3+}

ions (R = Pr and Nd), the transition temperature into the insulating state coincides with the antiferromagnetic ordering temperature, ($T_N = T_{IM}$), whereas, for the other members of the $RNiO_3$ series, these parameters are substantially different with $T_{IM} \gg T_N$ [2]. Recently, the insulator $\rightarrow$ metal transition was investigated by a resonant x-ray scattering experiment on $NdNiO_3$ single crystals [5, 6]. These experiments gave clear evidence for a first-order structural phase transition at T_{IM}, which has been attributed to the charge-ordering transition at the Ni sites [6].

Neutron diffraction and high-resolution synchrotron x-ray diffraction studies [7, 8] have recently shown that nickelates with small ions R^{3+} (Ho $\rightarrow$ Lu, Y) undergo a slight monoclinic distortion (space group $P2_1/n$) at temperatures $T \leqslant T_{IM}$, which implies the formation of two types of octahedral site for nickel cations: the larger [Ni(1)O_6] polyhedra with $\langle$Ni(1)–O$\rangle$ = 2.02 Å and the smaller [Ni(2)O_6] polyhedra with the average bond length $\langle$Ni(2)–O$\rangle$ = 1.92 Å. On the basis of these data, it was assumed, for the first time, that the transition into the insulating state ($T < T_{IM}$)—for nickelates with small rare-earth ions ($R^{3+} < 1.075$ Å)—was associated with a partial charge disproportionation $2Ni^{3+} \rightarrow Ni^{(3+\sigma)+} + Ni^{(3-\sigma')+}$, where $0 \leqslant \sigma(\sigma') \leqslant 1$ is the degree of the disproportionation [7]. However, Zhou *et al* [9] suggested that instead of a real charge transfer between NiO_6 octahedra, a segregation into ionic Ni^{3+}–O bonding, corresponding respectively to Jahn–Teller (JT) distorted Ni(1)O_6 octahedra and less distorted Ni(2)O_6 sites with covalent Ni^{III}–O bonding, leading to a long-range charge order along the crystallographic axis, could take place.

Analysis of the available experimental and theoretical data shows that a similar disproportionation process is also possible for the nickelates of medium-sized ions R^{3+} = Sm, Eu, Dy, and Gd [10]. One of the reasons for this assumption is that the nickelates $RNiO_3$ with R = Sm $\rightarrow$ Lu are characterized by $T_{IM} \neq T_N$ as also observed for the $RNiO_3$ perovskites (R = Ho $\rightarrow$ Lu). The disproportionation phenomenon seems progressively more difficult to detect by diffraction methods, since the characteristic monoclinic β angle becomes closer to 90° as the distortion of the perovskite is reduced, and taking into account that diffraction phenomena are mainly appropriated to study macroscopic effects with long-range ordering.

Although the physico-chemical properties of the above compounds have been intensively studied during the last 15 years, the questions of the nature of their ground electronic state and the local origin of the insulator–metal transition remain still open. Mössbauer spectroscopy involves local analysis; consequently, such a characterization could be more appropriate to follow this kind of electronic phenomenon. In fact, such a characterization has been recently developed for studying the local structure of perovskite nickelates [11–13].

The Mössbauer spectra of iron-doped samples $RNi_{0.98}Fe_{0.02}O_3$ (R = Lu, Y, Tl) measured at $T_N < T < T_{IM}$ were found to consist of a superposition of two quadrupole doublets Fe(1) and Fe(2), corresponding to the trivalent iron cations substituted for nickel in two different octahedral positions Ni(1)O_6 and Ni(2)O_6, respectively. The hyperfine parameters characterizing the Fe(1) and Fe(2) subspectra adequately reflect the specific features corresponding to the local Ni(1) and Ni(2) crystallographic sites [13]. On the other hand, the ^{57}Fe spectra of large rare-earth (R = Nd, Pr) nickelates showed the existence of only one Fe^{3+} site, thus underlying the absence of any disproportionation process for NiO_6 subarray [11].

The aim of this present work is to evaluate if Mössbauer spectroscopy is able to detect the charge disproportionation effect in $RNiO_3$ lattices with intermediate sizes of the rare-earth cations (R = Sm, Eu, Dy, Gd). Isotope ^{57}Fe was used as local probe to investigate the $RNi_{0.98}Fe_{0.02}O_3$ perovskites. This group of nickelates is of the greatest interest: they exhibit orthorhombic symmetry at $T > T_{IM}$, but their local structures in the temperature range $T_N < T < T_{IM}$ have remained questionable.

2. Experimental details

The main objective of the synthetic part of this work was to make the distribution of ^{57}Fe probe atoms into the nickelate structure as homogeneous as possible. The $RNi_{0.98}Fe_{0.02}O_3$ (R = Sm, Eu, Gd, Dy) samples were prepared through a high oxygen pressure treatment of precursors obtained from sol–gel preparation. Appropriate amounts of R_2O_3 (R = Sm, Eu, Gd, Dy) and $Ni(NO_3)_2{\cdot}6H_2O$ were dissolved in citric acid; a stoichiometric amount of metal ^{57}Fe was previously dissolved in 5 cm^3 of HNO_3 with some droplets of HCl and then added to the citrate solution. The mixtures of citrate and nitrate solutions were slowly evaporated, leading to organic resins, which were dried and decomposed by slowly heating up to 700 °C in air, for 12 h. This treatment gave rise to highly reactive precursor materials, amorphous according to x-ray diffraction. For each compound, the precursor powder was mixed and thoroughly ground with $KClO_4$ (30% in weight), put into a gold capsule (8 mm diameter, 10 mm length), sealed and placed in a cylindrical graphite heater. The reaction was carried out in a piston–cylinder press (Rockland Research Co.), at a pressure of 2 GPa at 900 °C for 20 min. Then the material was quenched to room temperature and the pressure was subsequently released. The product was ground and washed in a dilute HNO_3 aqueous solution, water being able to dissolve KCl resulting from the decomposition of $KClO_4$, and HNO_3 to eliminate small amounts of unreacted NiO, R_2O_3 and $R_2O_2CO_3$ impurity phases. Then the powder samples were dried in air at 150 °C for 1 h.

In order to evaluate if the oxygen pressure value plays a role on the distribution of the ^{57}Fe probe atoms in the nickelates lattice, the perovskite $GdNi_{0.98}Fe_{0.02}O_3$ was prepared according to a second method, which consisted of a two-step process. In the first step, nickel and iron hydroxides were coprecipitated by a 3 M KOH solution from an acid solution of a stoichiometric mixture of Ni(II) and ^{57}Fe(III) salts. The resulting homogeneous hydroxide mixture was washed, dried and annealed in air at 300 °C until the formation of the ^{57}Fe-doped nickel oxide precursor '$Ni_{0.98}Fe_{0.02}O$'. At the second step a stoichiometric mixture of Gd_2O_3 and $Ni_{0.98}Fe_{0.02}O$ precursors with the addition of $KClO_3$ as oxygen source (20–30% in weight) was treated under high-pressure conditions (6 GPa, 900 °C, 10 min) in a belt-type equipment. The resulting KCl was rapidly leached out with distilled water.

The x-ray powder diffraction patterns at 300 K ((figure 1) for $EuNiO_3$: ^{57}Fe (2%)) and chemical analysis of the final products obtained from both processes demonstrated the lack of impurity phases and the formation of samples with an orthorhombic (space group *Pbnm*) lattice.

The ^{57}Fe Mössbauer spectra were recorded at 300 K using a conventional constant acceleration Mössbauer spectrometer. The radiation source ^{57}Co(Rh) was maintained at room temperature. All isomer shifts refer to the α-Fe absorber at 300 K. The method of restoration of a distribution function of the hyperfine parameter of a partial spectrum [15] has been used for processing and analysing the Mössbauer spectra. The method is realized in the DISTRI computer code of the package *MS* Tools [15].

3. Method for reconstructing distribution functions of Mössbauer spectral parameters

In the case of a locally inhomogeneous system, the line shape of the experimental Mössbauer spectrum, $N_{\rm th}(\{a^{\rm s}\}, \{P^{\rm s}\})$, can be described as a superposition of separate components [14, 15]:

$$N_{\rm th}(\{a^{\rm s}\}, \{P^{\rm s}\}) = N_\infty - \sum_{s=1}^{t} D(a^{\rm s})P^{\rm s} \tag{1}$$

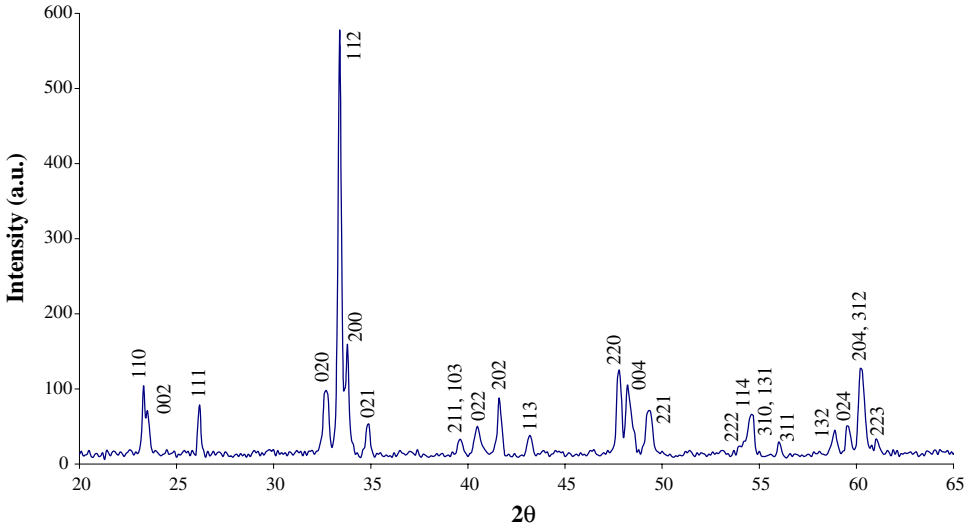

Figure 1. X-ray diffraction spectrum for $EuNiO_3$: ^{57}Fe (2%) as an illustration of the synthesis process.

(This figure is in colour only in the electronic version)

where $\{a^s\}$ is the set of varied hyperfine parameters; $\{P^s\}$ is the set of distribution functions of these parameters ($s = 1, 2, \ldots, t$); t is the total number of distribution functions; $N_\infty = N_0 + c(v_j - v_0)^2$ is the baseline taking into account a probable 'geometrical' effect (v_j is the Doppler velocity corresponding to the jth experimental point); $D(a^s)$ is the matrix describing a nucleus of the sth distribution function and is immediately related to the hyperfine parameters as

$$D(a^s) \equiv D_{jk}(a^s) = \sum_{l=1}^{6} A_l^s \cdot Z(v_j; v_{kl}^s, \Gamma^s) \tag{2}$$

where $Z(v_j; v_{kl}^s, \Gamma_k^s)$ is the function describing the line shape of the resonant line ($j = 1, 2, \ldots, n$; $k = 1, 2, \ldots, r^s$); A_l^s, $v_{k,l}^s$, and Γ_k^s are the amplitude, position, and width of the lth component in a partial spectrum with hyperfine parameters δ_k^s, ε_k^s, and H_k^s. The width Γ_k^s of the partial spectrum components is represented as a sum of the source linewidth Γ_s, natural linewidth Γ_τ, and additional width $\delta\Gamma_k^s$.

In the DISTRI code the search for the distribution function $\{P^s\}$ of the hyperfine parameters δ_k^s, ε_k^s, H_k^s, and $\delta\Gamma_k^s$ of the sth partial spectrum suggests a linear correlation between them so that the parameters δ_k^s, ε_k^s, H_k^s, and $\delta\Gamma_k^s$ are defined only by origins (δ^s, ε^s, H^s, and $\delta\Gamma^s$) and values ($\Delta\delta^s$, $\Delta\varepsilon^s$, ΔH^s, and $\Delta\delta\Gamma^s$) of intervals of their values for each s-distribution.

The problem of reconstructing the $\{P^s\}$ functions can be solved by one of the methods for solving incorrect problems [16]. The method is based on a generalized interactive regularization. As the functional to be minimized, a composite functional is taken, which contains, except for the contribution

$$\chi_{sp}^2(\{a^s\}, \{P^s\}) = \|S_N^{-1} \otimes [N_{exp} - N_{th}(\{a^s\}, \{P^s\})]\|_n^2, \tag{3}$$

defined by the discrepancy between the experimental spectrum N_{exp} and the assumed line shape N_{th}, two more regularizing contributions:

$$\chi_u^2(\{a^s\}, \{P^s\}) = \sum_{s=1}^{t} u^s \|(\sigma_s^{-1} \otimes T^s) P^s\|_r^2, \tag{4}$$

$$\chi^2_{\omega}(\{a^s\},\{P^s\}) = \sum_{s=1}^{t} \omega^s \|\sigma_s^{-1} \otimes (p^s - P^s)\|_r^2, \tag{5}$$

where the $\{S_N\}$ are standard deviations of statistical errors in the spectrum; n is the number of experimental points in the spectrum; the $\{T^s\}$ are matrices of finite differences, defined by the degree of a derivative, according to which regularization is carried out; the $\{p^s\}$ are the distributions of parameters, expected by *a priori* data; the $\{\sigma^s\}$ are the regularization 'rigidities' at the points of distribution representation, having the meaning of standard deviations; the $\{u^s\}$ and $\{\omega^s\}$ are regularization parameters; and the $\{r^s\}$ are dimensions of distribution functions.

Using the contribution $\chi^2_u(\{a^s\},\{P^s\})$, conditions are imposed on the smoothness of one of the derivatives (up to the tenth order) of functions $\{P^s\}$ at the reconstruction. The smoothness is set by regularization parameters $\{u^s\}$ and rigidities $\{\sigma^s\}$. The greater the $\{u^s\}$ and the lower the $\{\sigma^s\}$, the more rigid is the requirement for derivative smoothness within the given interval. Regularization, non-uniform along representation points, allows us to take into account *a priori* data on local maxima of the distribution for some value at a certain reconstruction stage.

The contribution $\chi^2_{\omega}(\{a^s\},\{p^s\})$ is intended for a direct use of assumed values $\{p^s\}$ of functions $\{P^s\}$ found by other methods or at earlier reconstruction stages. Confidence of these *a priori* data as a whole and in each interval separately is taken into account using regularization parameters $\{\omega^s\}$ and rigidities $\{\sigma^s\}$. The higher the confidence, the greater the $\{\omega^s\}$ and the lower the $\{\sigma^s\}$.

An important and noteworthy aspect of applying the DISTRI code to reconstruct the distribution $P(v)$ of shifts for a solitary resonant line (hyperfine structure component) and the reconstruction result can be considered to be the growth in spectral resolution compared to linear methods [17].

4. Results and discussions

Figure 2 shows the ^{57}Fe Mössbauer spectra of the $RNi_{0.98}Fe_{0.02}O_3$ (R = Sm, Eu, Dy) samples measured at $T_N < T < T_{IM}$.

First, the distribution functions $P(v)$ of the positions of individual Lorentzian lines were restored. For the Sm nickelate the $P(v)$ function is asymmetric and such an asymmetry is transformed to two distinct peaks when the R^{3+} ionic radius is decreasing. Consequently the $P(v)$ profile for the nickelates R = Sm, Eu, or Dy, which exhibit insulator properties ($T < T_{IM}$), can be described as a superposition of two symmetric peaks of the same width at half-maximum ($\Gamma_{1,2} \approx 0.1$ mm s^{-1}) but of different intensities ($I_1/I_2 \approx 2$). The distance between these peaks monotonically increases on decreasing the radius of the R^{3+} cation (Sm $\rightarrow$ Dy).

The asymmetry of the $P(v)$ profile can be induced by several factors: (i) the presence of a small amount of impurity phases, which are not detected by the x-ray powder diffraction method; (ii) the Goldanskii–Karyagin effect related to the anisotropy of thermal vibrations of iron dopant atoms [18]; (iii) the presence of texture in fine crystalline samples, which results in the angle dependence of the nuclear transitions $\pi_{(\pm 3/2 \rightarrow \pm 1/2)}$ and $\sigma_{(\pm 1/2 \rightarrow \pm 1/2)}$ [19]; and (iv) a superposition of two subspectra corresponding to two non-equivalent iron positions in the nickelate structures.

An analysis of these different factors is able to explain such an asymmetry, and leads to the following conclusions.

- Firstly, the presence of reproducible impurity phases is unlikely since the nickelates with different R^{3+} ions were synthesized under different experimental conditions. In addition, our preliminary Mössbauer measurements in the temperature range of magnetic ordering

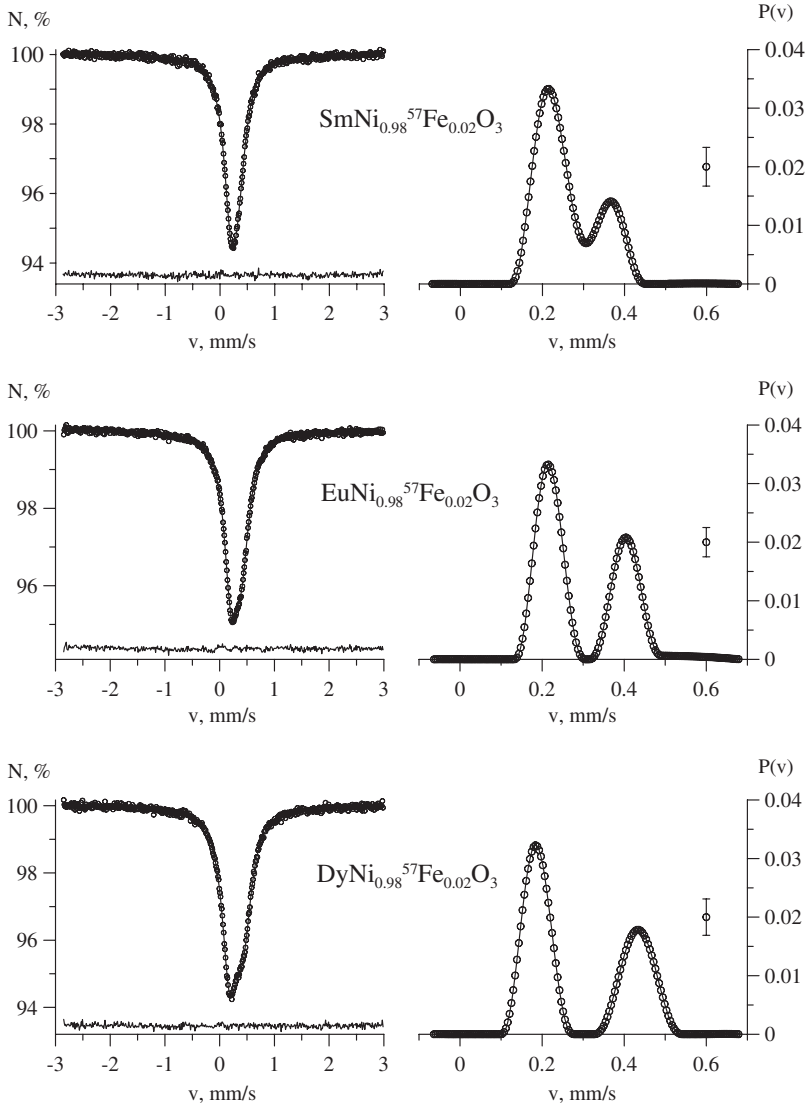

Figure 2. ^{57}Fe Mössbauer spectra and corresponding distribution functions $P(v)$ for the nickelates $RNi_{0.98}Fe_{0.02}O_3$ at $T_s = 300$ K ($T_N < T < T_{IM}$). (The lower traces below the Mössbauer spectra correspond to the differences between observed and calculated spectra.)

($T < T_N$) showed that all the paramagnetic components are simultaneously converted into magnetic Zeeman sextets at $T = T_N$, which confirms that they belong to the matrix of the same compound.

- Secondly, the Goldanskii–Karyagin effect is also hardly probable because of a high symmetry of the local environment of the ^{57}Fe dopant atoms, which is reflected by a small quadrupole splitting value corresponding to the distance between the two peaks in the restored distribution $P(v)$ functions.
- Thirdly, in order to check the possibility of a specific local crystal texture, we measured the spectrum of one of the samples (R = Dy) at the angle $\vartheta = 54.7°$ between the normal

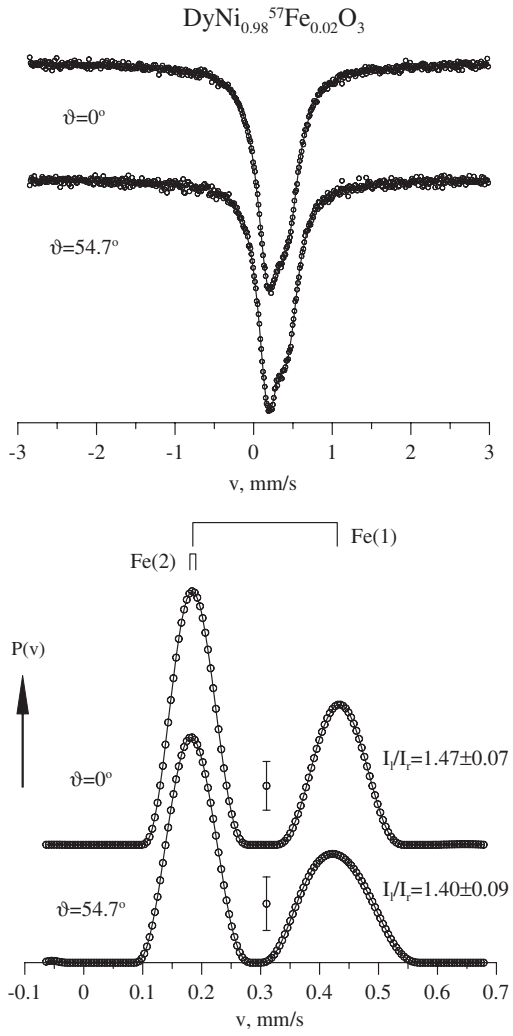

Figure 3. ^{57}Fe Mössbauer spectra and distribution functions $P(v)$ for the $DyNi_{0.98}Fe_{0.02}O_3$ sample recorded at different angles (ϑ) between the normal to its plane and the γ-ray direction. The lines above the $P(v)$ functions show a model deconvolution of the experimental spectrum using two quadrupole doublets (see text).

to its plane of the sample holder and the γ-ray direction, at which the texture does not contribute to the spectrum [19]. The lack of visible changes in the relative intensities of $P(v)$ distribution components (figure 3) allows us to rule out the texture of the samples.

- Finally, the most plausible reason explaining the observed asymmetry of the $P(v)$ profile for the nickelates with intermediate rare earths (R = Sm, Eu, Gd, and Dy) is that ^{57}Fe dopant atoms would be simultaneously stabilized in two non-equivalent crystallographic positions. It is worth noting that the considerable difference between the positions of the two peaks ($\approx$0.4 mm s^{-1}) excludes the possibility that each of these peaks corresponds to an individual state of iron cations within the nickelate structures. This conclusion is also consistent with the surmise that iron cations in strongly different electronic states cannot be simultaneously characterized by precisely the same quadrupole splitting values (the ratio of the corresponding line widths at half-maximum is $\Gamma_1/\Gamma_2 \approx 1$). Therefore, only one model remains valid, namely, the model of representation of experimental spectra as a superposition of the quadrupole doublet Fe(1) with higher δ_1 and Δ_1 values and the

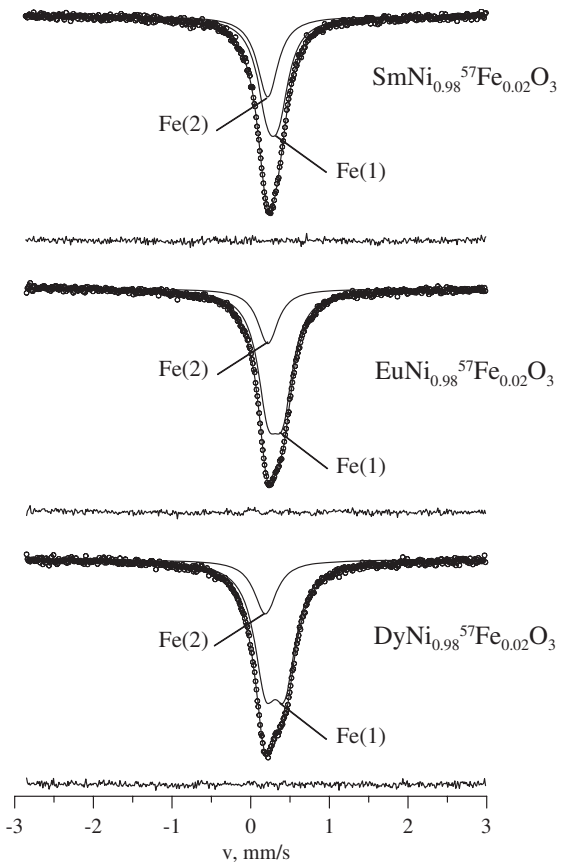

Figure 4. ^{57}Fe Mössbauer spectra of R = Sm, Eu, Dy nickelates described as a superposition of the two quadrupole doublets.

virtually unresolved doublet Fe(2) with smaller isomer shift (δ_2) and quadrupole splitting (Δ_2) values. The spectra described in the framework of this 'discrete' model are shown in figure 4.

Analysis of the hyperfine ^{57}Fe parameters thus obtained (figure 5) allows us to draw the following conclusions.

Firstly, the general pattern of the subspectra of Fe(1) and Fe(2) is closely comparable to the spectra of the nickelates $RNi_{0.98}Fe_{0.02}O_3$ (R = Lu, Y, Tl) with the monoclinic structure at $T_N < T < T_{IM}$, where the Fe^{3+} probe ions substituted for nickel in the [Ni(1)O_6] and [Ni(2)O_6] polyhedra [11–13]. This similarity allows us to assume that, due probably to a slight monoclinic distortion of the crystal structures of the nickelates R = Sm, Eu, Gd, and Dy undetectable by diffraction analysis, these perovskites contain two types of octahedral position, Ni(1) and Ni(2), which are partially substituted by the ^{57}Fe dopant atoms Fe(1) and Fe(2), respectively.

Secondly, the isomer shifts values observed for both iron states correspond to the formal trivalent ferric ions in the oxide compounds [20]. The difference observed between δ_1 and δ_2 values can be associated with the different character of Fe–O chemical bonds in both [$Fe_{(i)}O_6$] polyhedra. Taking into account that a decrease in the Fe–O distance normally leads to an increase of the M–O covalency, such a phenomenon is associated with a decrease of the corresponding isomer shift. Consequently, the quadrupole doublet with higher δ_1 value can be assigned to the Fe(1) ions substituted for nickel in larger [Ni(1)O_6] octahedra. In this

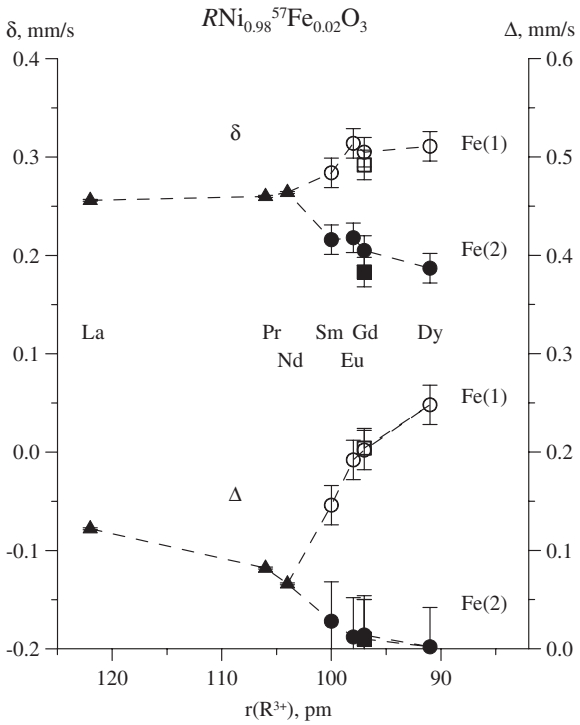

Figure 5. ^{57}Fe hyperfine parameters of $RNi_{0.98}Fe_{0.02}O_3$ spectra described in the framework of the 'discrete' model (S_1 and S_2 are respectively the surfaces of the subspectra corresponding to Fe(1) and Fe (2)). For the ^{57}Fe: ▲ δ value for $RNi_{0.98}Fe_{0.02}O_3$ perovskites without disproportionation. ● δ_1 value and ○ δ_2 value for $RNi_{0.98}Fe_{0.02}O_3$ perovskites with disproportionation. ■ δ_1 value and □ δ_2 value for the $GdNi_{0.98}Fe_{0.02}O_3$ prepared in different pressure conditions.

case, the second doublet with the smaller δ_2 should arise from the Fe(2) ions substituted for nickel in the small Ni(2)O_6 octahedra. We can assess how much the experimental difference between δ_2 and δ_1 is consistent with the expected difference between the average bond lengths $\langle$Fe(i)–O$\rangle$ in the [Fe(1)O_6] and [Fe(2)O_6] polyhedra. To do this, we assume that the difference between the $\langle$Fe(1)–O$\rangle$ and $\langle$Fe(2)–O$\rangle$ bond lengths is equal to 0.08 Å, which corresponds to the difference between the average bond lengths in the [Ni(2)O_6] and [Ni(1)O_6] polyhedra in the unsubstituted nickelates $RNiO_3$ (R = Ho–Lu, Y) with monoclinic structures [7, 8]. Using the value $\partial\delta/\partial R_{Fe-O} = 1.18$ mm s^{-1} Å^{-1}, from [21], we obtain the expected difference in isomer shifts $\Delta\delta = (\partial\delta/\partial R_{Fe-O}) \times 0.08 = 0.09(\pm 0.01)$ mm s^{-1}, which is in good agreement with the experimental value $\langle\delta_1–\delta_2\rangle = 0.10$ mm s^{-1}.

Thirdly, taking into account that the main component (q) of the electric field gradient (EFG) at the nuclei of the Fe^{3+}: $3d^5(^6S_0)$ ions with the isotropic electronic configuration is caused by a distortion of their crystallographic environment, the observed difference between the Δ_1 and Δ_2 values ($\Delta_i = e^2 q_{(i)} Q$, where Q is the quadrupole moment of the ^{57}Fe nucleus in the first excited state) is due to the considerable difference between the local distortions of the [Fe(1)O_6] and [Fe(2)O_6] polyhedra. This result is in qualitative agreement with the neutron diffraction data for undoped $RNiO_3$ nickelates (R = Ho–Lu, Y), which indicate that [Ni(1)O_6] polyhedra are more distorted than the [Ni(2)O_6] ones [20]. Unfortunately, the small partial contribution of the Fe(1) component (figure 3), which leads to a large error in the determination

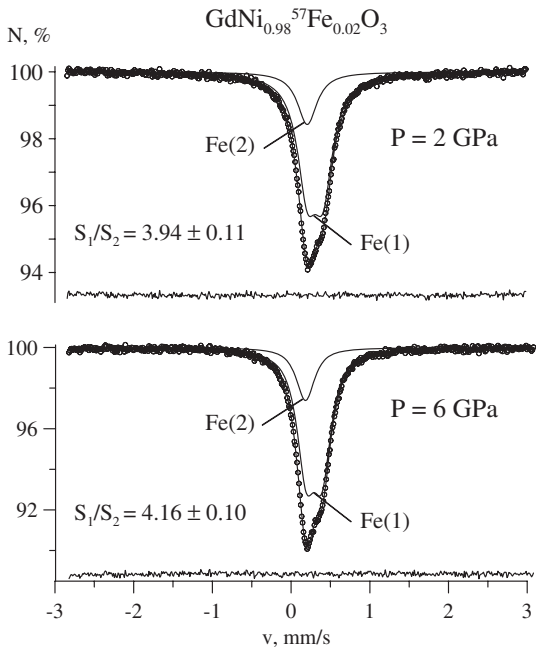

Figure 6. ^{57}Fe Mössbauer spectra of the $GdNi_{0.98}Fe_{0.02}O_3$ nickelate prepared by two different methods.

of the Δ_1 value, hinders reliable semiquantitative estimates that would make it possible to correlate the experimental quadrupole splittings $\Delta_{1(2)}$ with the geometry of the Fe(1) and Fe(2) local environments.

Fourthly, the ratio of the Fe(1) and Fe(2) subspectrum areas differs considerably from unity, thus pointing to the lack of a random distribution of the iron dopant cations over the two crystallographic positions of the nickelate lattice. One possible reason for this can be 'steric' effects related to the fact that the size of $[Fe^{3+}O_6]$ octahedral polyhedra in ferric oxide compounds ($\langle Fe^{3+}–O\rangle \approx 2.03$ Å [22]) is close to the size of the $[Ni(1)O_6]$ polyhedra in monoclinic $RNi_{0.98}Fe_{0.02}O_3$ ($\langle Ni(1)–O\rangle \approx 2.00$ Å). This seems to be responsible for the preferable substitution of trivalent iron for the Ni(1) cations as compared to the Ni(2) cations, which are located in the considerably smaller $[Ni(2)O_6]$ polyhedra ($\langle Ni(2)–O\rangle \approx 1.92$ Å). It may seem unexpected that the ratio of the areas of the two subspectra remains virtually constant within the error of measurement ($I_1/I_2 \approx 2$) for nickelates with different degrees of monoclinic distortion. However, this result is in good agreement with the data in [19], which demonstrate that the effective charges of the Ni(1) and Ni(2) cations and, hence, the sizes of the $[Ni(1)O_6]$ and $[Ni(2)O_6]$ polyhedra remain virtually unaltered with an increase in the degree of monoclinic distortion in nickelates $RNiO_3$ (Ho → Lu, Y).

In order to evaluate if the preparation method could play a role on the Mössbauer study, two spectra are given for the same $GdNi_{0.98}Fe_{0.02}O_3$ composition of samples prepared by two different methods (figure 6), described in section 2. (S_1 and S_2 are respectively the surfaces of the subspectra corresponding to Fe(1) and Fe(2).) No detectable differences being observed, it can be concluded that the preparation method could not play a role in the distribution of the ^{57}Fe probe atoms in the nickelate lattices.

It is worth noting that, in our previous works [11–13], the spectrum of $SmNi_{0.98}Fe_{0.02}O_3$ measured in the temperature range $T_N < T < T_{IM}$ was represented by one unresolved quadrupole doublet. This allowed us to conclude that all Fe^{3+} probe ions in this nickelate are in equivalent crystallographic positions. However, in the present work, the spectra were measured

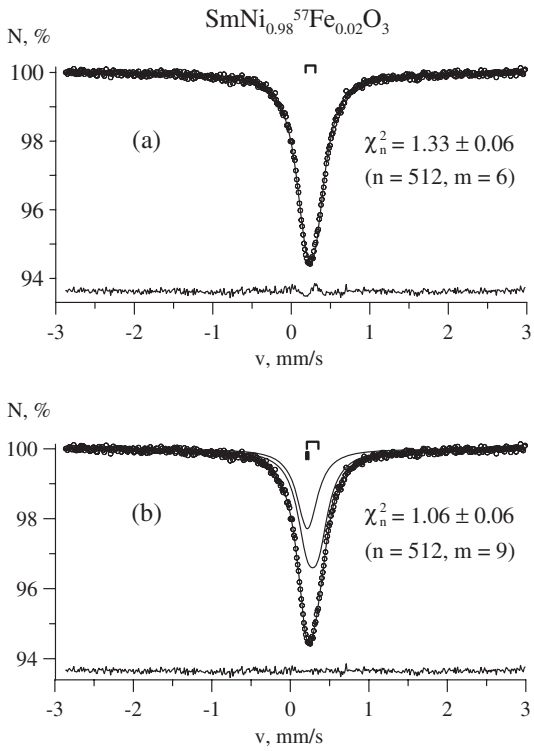

Figure 7. ^{57}Fe Mössbauer spectra of the $SmNi_{0.98}Fe_{0.02}O_3$ nickelate described by two different models (the quadrupole splittings are indicated above each figure: (a) for the Mössbauer spectrum before deconvolution, (b) for each subspectrum).

with larger statistics and resolution, which make it possible to use more rigorous statistical methods to assess the quality of the model description of the experimental spectrum. For example, figure 7 shows two models of decomposition of the spectrum of $SmNi_{0.98}Fe_{0.02}O_3$: (i) as a single quadrupole doublet (figure 6(a)); and (ii) as a superposition of two quadrupole doublets (figure 6(b)). In each case, the quality of the mathematical deconvolution of a experimental spectrum was estimated using the reduced χ_n^2 function ($\chi_n^2 = \chi^2/r$), which takes into account not only the degree of the discrepancy between the experimental spectrum and the model spectrum (χ^2) but also the number of the degrees of freedom $r = (n - m)$ (n is the number of experimental data points in the spectrum, m is the number of parameters varied during the fit). When the spectrum is represented by a superposition of two quadrupole doublets (figure 6(b)), no systematic deviations between the experimental Mössbauer data and the model spectrum are observed, and the corresponding χ_n^2 value is considerably lower than the value obtained in [11–13] for a single unresolved doublet (figure 6(a)). This result confirms that the second model used for the analysis of the $SmNi_{0.98}Fe_{0.02}O_3$ spectrum is more appropriate to describe the experimental data. Consequently, it was concluded that Fe^{3+} cations, in the $SmNi_{0.98}Fe_{0.02}O_3$ lattice, are stabilized in two closely spaced positions, which are distinguished by their hyperfine parameters.

5. Conclusion

The above experimental data illustrate the efficiency of Mössbauer spectroscopy as a local probe that provides important information on the microstructure of perovskite-like nickelates, compared to other characterization techniques more appropriate for studying macroscopic

phenomena. In particular, the first indirect evidence has been obtained for the existence of two types of nickel position in the perovskite $RNiO_3$ structures with R = Sm, Eu, Dy, and Gd at $T < T_{IM}$, which remained indiscernible to diffraction methods. This result underlines the role of structural and electronic factors responsible for the metal–insulator transition. In particular, we may state that, at $T_N < T < T_{IM}$, the lattices of the nickelates with R = Sm → Lu, Y, and Tl are characterized by two types of non-equivalent nickel position, $[Ni(1)O_6]$ and $[Ni(2)O_6]$, with different geometric parameters and electronic structures, which arise from the structural distortion caused by the electron–lattice interaction [10] or by the charge disproportionation or charge ordering in the nickel sublattice [7, 8]. In order to get more information concerning the evolution of the T_{IM} value versus the R^{3+} cation, a Mössbauer study of $RNi_{0.98}Fe_{0.02}O_3$ series at $T \geqslant T_{IM}$ (where the nickelates exhibit metallic conductivity) is in progress.

Acknowledgments

The authors would like to acknowledge financial support by the Russian Foundation for Basic Research (RFBR-CNRS Ref No 05-03-22003), the French Research Agency CNRS (PICS 3200) and the French Ministry for Foreign Affairs for supporting a Thesis in co-tutelle (AB) and the Spanish Ministry of Education through the Project MAT2004-0479. We also thank INTAS (Ref No 03-55-2453) for supporting AB.

References

[1] Lacorre P, Torrance J B, Pannetier J, Nazzal A I, Wang P W and Huang T C 1991 *J. Solid State Chem.* **91** 225
[2] Garcia-Munoz J L, Rodriguez-Carvajal J, Lacorre P and Torrance J B 1992 *Phys. Rev.* B **46** 4414
[3] Kim S J, Demazeau G, Alonso J A, Largeteau A, Martinez-Lope J M, Presniakov I and Choy J H 2000 *Solid State Commun.* **117** 113
[4] Torrance J B, Lacorre P, Nazzal A I, Ansaldo E J and Niedermayer C 1992 *Phys. Rev.* B **45** R8209
[5] Zaghrioui M, Bulou A, Lacorre P and Laffez P 2001 *Phys. Rev.* B **64** 081102(R)
[6] Staub U, Meijer G I, Fauth F, Allenspach R, Bednorz J G, Karpinski J, Kazadov S M, Paolasini L and d'Acapito F 2002 *Phys. Rev. Lett.* **88** 126402
[7] Alonso J A, Martinez-Lope J M, Casais M T, Aranda M A G and Fernadez-Diaz M T 1999 *J. Am. Chem. Soc.* **121** 4754
[8] Alonso J A, Martinez-Lope J M, Casais M T, Garcia-Munoz J L, Fernandez-Diaz M T and Aranda M A G 2001 *Phys. Rev.* B **64** 094102
[9] Zhou J S and Goodenough J B 2005 *Phys. Rev.* B **69** 153105
[10] Alonso J A, Martinez-Lope M J, Casais M T, Martinez J L, Demazeau G, Largeteau A, Garcia-Munoz J L, Munoz A and Fernandez-Diaz M T 1999 *Chem. Mater.* **11** 2463
[11] Kim S J, Demazeau G, Presniakov I, Pokholok K, Sobolev A and Ovanesyan N 2001 *J. Am. Chem. Soc.* **123** 8127
[12] Kim S J, Demazeau G, Presniakov I, Pokholok K, Baranov A, Sobolev A, Pankratov D and Ovanesyan N 2002 *Phys. Rev.* B **66** 014427
[13] Kim S J, Presniakov I, Demazeau G, Pokholok K, Baranov A, Sobolev A, Pankratov D and Ovanesyan N 2002 *J. Solid State Chem.* **168** 12
[14] Rusakov V S 1999 *Izv. Ross. Acad. Nauk, Ser. Fiz.* **63** 1389
[15] Rusakov V S and Chistyakova N I 1992 *Mössbauer Program Complex MSTools LACAME'92* (Argentina: Buenos Aires)
[16] Karyagin S V 1963 *Proc. Acad. Sci. USSR. Phys. Chem. Sect.* **148** 110
[17] Karyagin S V 1964 *Sov. Phys.—Solid State* **5** 1552
[18] Menil F 1985 *J. Phys. Chem. Solids.* **46** 763
[19] Sawatzky G A and Van der Woude F 1974 *J. Phys. Coll.* **35** C6 47
[20] Alonso J A, Martinez-Lope M J, Casais M T, Garcia-Munoz J L and Fernandez-Diaz M T 2000 *Phys. Rev.* B **61** 1756
[21] Shannon R D 1976 *Acta Crystallogr.* A **32** 751
[22] Shannon R D and Prewitt C T 1969 *Acta Crystallogr.* B **25** 925